Journal of Solid State Chemistry **162,** 270–281 (2001)
doi:10.1006/jssc.2001.9293, available online at http://www.idealibrary.com on IDEAL®

The Outcome of Cobalt in the Nickel–Cobalt Oxyhydroxide Electrodes of Alkaline Batteries

V. Pralong, A. Delahaye-Vidal, Y. Chabre,* B. Beaudoin, and J.-M. Tarascon

Laboratoire de Réactivité et de Chimie des Solides, Université de Picardie Jules Verne and CNRS, 33 rue St. Leu, 80039 Amiens, France; and
**Laboratoire de Spectrométrie Physique, Université Joseph Fourier-Grenoble I and CNRS, BP 87, 38402 St. Martin d'Hères, France*

Received February 27, 2001; in revised form June 26, 2001; accepted July 2, 2001

IN HONOR OF PROFESSOR PAUL HAGENMULLER ON THE OCCASION OF HIS 80TH BIRTHDAY

The evolution of cobalt hydroxide used as a coating for nickel hydroxide electrodes has been studied as a function of the redox potential window and upon cycling. From both chemical and electrochemical studies, it is shown that (i) upon deep discharges cobalt tends to migrate from the coating to the current collector and (ii) upon heavy cycling in the limited 1–1.4 V potential range a complete reorganization of the active material occurs. In the latter case, using X-ray diffraction, electron microscopy, and potentiodynamic intermittent technique, we identified the formation of a $Ni_{1-x}Co_x(OH)_2(CO_3)_z \cdot rH_2O$-type phase through dissolution reprecipitation processes involving both cobalt and nickel species. From these findings, the conditions required to preserve the benefits of cobalt additives are given. © 2001 Elsevier Science

***Key Words*: nickel hydroxide; nickel oxyhydroxide; cobalt hydroxide; NiOOH; $Ni(OH)_2$; $Co(OH)_2$; potentiodynamic techniques.**

INTRODUCTION

Secondary Ni-based alkaline batteries are widely used in today's portable applications and intense efforts to improve their specific capacity are still being made. A new composite positive electrode called "high density" has appeared recently in commercial batteries. This improved composite electrode consists of spherical β-nickel hydroxide particles coated with cobalt hydroxide. Such a coating was shown to provide, among the most pronounced beneficial effects, a minimization of the γ-NiOOH growth at the nickel oxide electrode (NOE) during charging (1–3) and an enhanced nickel electrode conductivity (4–6) together with an increase in NOE capacity.

Although much research has been focused on the improvement of the Co-coating-driven NOE electrode, little work has been devoted to its fundamental origin. According to Oshitani *et al.* (4), the divalent cobalt-based precursor dissolves in the electrolyte forming a deep blue complex, and CoOOH reprecipitates around the platelets of the nickel hydroxide enabling a good electrical path between them. Later, Delmas *et al.* (5) showed that these improvements were nested in the presence of a highly conductive CoOOH-type phase formed by oxidation of the cobalted precursor. Recently, we reported (6, 7) the electrochemical behavior of $Co(OH)_2$ in alkaline media and showed the production, depending on the first charging rate (e.g., oxidation rate), of cobalt oxyhydroxide having different textures and electrochemical signatures with, for instance, the formation of a highly conductive β-CoOOH′ phase containing Co^{4+} for charging rates greater than C/10. We further demonstrated that the electronic benefits of this highly conductive phase (high cycling efficiency) are preserved if, during cycling, the cutoff discharge voltage is maintained above 1 V (e.g., above 0.7 and 0 V corresponding to the reduction of CoOOH into β-$Co(OH)_2$ and of β-$Co(OH)_2$ into Co^0, respectively).

However, to ensure the practical relevance of our previous findings a key issue resided in determining whether the electrochemical behavior of $Co(OH)_2$ was preserved in the presence of a nickel hydroxide environment. This paper, by focusing on a complete electrochemical study of the cobalt hydroxide post-added in the nickel oxyhydroxide electrode, addresses this key issue together with the outcome of Co (e.g., formation of an $Ni_{1-x}Co_x(OH)_2(CO_3)_z \cdot rH_2O$-type phase) within the NOE electrode upon cycling.

EXPERIMENTAL

X-ray diffraction (XRD) patterns were collected using a Philips diffractometer PW1710/1729 with CuK_a ($l = 0.15406$ nm). A scanning electron microscope (SEM) Field Effect Gun (FEG) Philips XL-30 with a resolution of about 1 nm was used to study textural changes while elemental compositions were determined by energy dispersive spectroscopy (EDS) on a Link-Isis analyzer (ATW 6650 detector).

0022-4596/01 $35.00

The sample morphologies were determined by means of a transmission electron microscope (TEM), Philips CM12 instrument.

The β-$Ni(OH)_2$ nickel hydroxide samples investigated in this study are homemade. First, we added a nickel nitrate solution (1 mol/L) to an ammonia solution (1 mol/L) at room temperature to obtain a turbostratic α-type nickel hydroxide as reported by Le Bihan and Figlarz (8). Then, this phase transformed into the β(II) material under hydrothermal conditions at around 125°C and 1.2 bars. Commercial cobalt hydroxide $Co(OH)_2$ precursor (UM Belgium) was used for the experiments. Both nickel and cobalt hydroxide crystallized in the *P*-3*m*1 space group and consisted of large monolithic platelets (around 200 to 1000 Å) showing Bragg extinction contours as determined by TEM observations.

The nickel oxyhydroxide electrode was made as follows: 65% of commercial cobalt hydroxide, 30% Super P carbon black (from M.M.M., Belgium) used as electronic binder, and 5% polytetrafluoroethylene (PTFE) used as mechanical binder were thoroughly mixed to form the active paste. The composite nickel–cobalt electrodes were prepared by inserting this paste into a 2.25-mm-thick nickel foam plate. These electrodes were dried at 50°C and cut into disks (1.14 cm^2), which were then pressed at about 2 tons/cm^2. For the negative electrode, 1.14-cm^2 disks were directly cut out from SAFT $Cd/Cd(OH)_2$ electrodes. Laboratory electrochemical test cells in PTFE (Swagelok-type; Ref. 9) were assembled with the positive electrode containing 24 mg of cobalt hydroxide (theoretical capacity, 7 mA.h) separated from the Cd negative electrode by a polyamide separator impregnated with 0.5 ml of a CO_2-free 5 N KOH solution (from Prolabo; Min, 34% aqueous solution). The electrochemical tests were carried out using an Arbin cycling system (Arbin Co., TX, USA) or a VMP system (Biologic S. A., Claix, France) that operates in both galvanostatic and potentiostatic modes. All the potentials given in this paper have been recorded versus $Cd/Cd(OH)_2$.

Cyclic voltammetry experiments were performed using a Pt electrode as the counter electrode, a mini glass carbon electrode (6.0805.010 Metrohm; diameter, 0.5 cm) as the working electrode, and a Hg/HgO electrode (XR440 from Radiometer-Copenhagen) as the reference electrode. The three electrodes were immersed in 10 mL of KOH solutions containing, or not, cobalt, nickel, and cobalt hydroxo complexes. The potential sweep was controlled by an Autolab potentiostat PGSTAT20 at a sweep rate of 5 mV/s. Before starting the sweep, the electrode was immersed for 10 min in the electrolyte solution under argon flow to stabilize the electrode potential.

RESULTS AND DISCUSSION

Study of the First Cycle of a Composite Electrode as a Function of the Discharge Cutoff Voltage

The potential versus time evolution values of NOE electrodes containing $Ni(OH)_2 + x$ wt% of $Co(OH)_2$ with $x = 0$, 10, and 25 were collected during the first charge with a C/10 galvanic rate. We observed (Fig. 1) that the amplitude of the 0.9-V signature, corresponding to the $Co^{2+} \rightarrow$

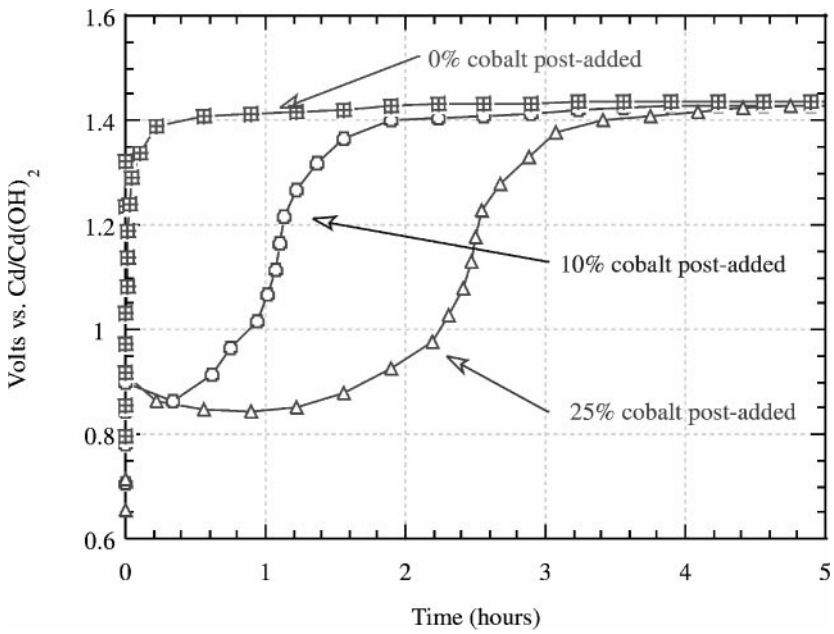

FIG. 1. First charge at a C/10 rate versus x in $NiOOH_{(1+x)}$ for different cobalt oxyhydroxide coating contents: 0, 10, and 25 wt%. Weight of active material, about 24 mg; theoretical capacity, 6.9 mAh; potential windows, 0.7 to 1.45 V.

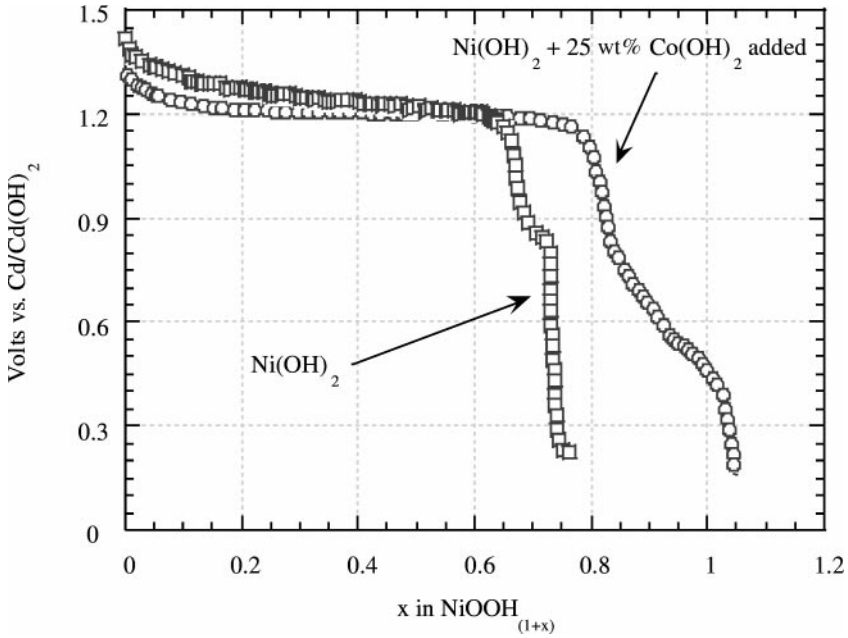

FIG. 2. First discharge at a C/10 rate versus x in $NiOOH_{(1+x)}$ for two different cobalt oxyhydroxide contents: 0 and 25 wt%. Weight of active material, about 24 mg; theoretical capacity, 6.9 mAh; potential windows, 1.45 to 0.2 V.

Co^{3+} oxidation reaction, is directly proportional to the cobalt amount in the electrode (3). On the basis of our previous work, we recall that charging an NOE industrial electrode that never contains more than 10 wt% of post-added cobalt hydroxide at a rate of C/10 leads to the formation of a highly conductive nonstoichiometric $Co_x^{4+}Co_{1-x}^{3+}OOH_{1-x}$ phase that turns out to be beneficial to the electrochemical efficiency of the NOE electrode.

Once charged the above Co-free and 25% Co-containing NOE electrodes were discharged at a C/20 rate. The discharge curve responses (Fig. 2) confirmed, as previously reported, some salient differences such as (1) the Co-driven enhancement of the NOE electrode performance and (2) the disappearance of the 0.8-V reduction plateau (frequently referred to as the second plateau) observed for Co-free NOE electrodes. Depending on the authors the origin of the latter effect is rooted either in the Co-driven disappearance of a certain type of crystallographic defects or in the decreasing amounts of the γ-NiOOH phase formed in Co-containing electrodes during charging (10).

Further differences appear between the Co-free and Co-containing NOE electrodes as the discharge voltage is lowered as shown in Fig. 2. Below 0.8 V, the voltage–time curve drops sharply for the Co-free NOE electrode while the Co-containing sample exhibits extra capacities over the 0.9–0.3 V range (Fig. 2). While the origin of the first capacity domain is still not understood, we can, based on our previous study of the electrochemical behavior of cobalt oxyhydroxide electrodes, unambiguously ascribe the origin of the extra capacity observed below 0.55 V to the CoOOH reduction onto $Co(OH)_2$. Through this previous study, we also showed that the $CoOOH \rightarrow Co(OH)_2$ reduction was followed by a Co^{2+} dissolution step and then by a cobalt hydroxide recrystallization preferentially occurring at the current collector surface. At this point, a legitimate question arises: Will the CoOOH reduction path reported for pure $Co(OH)_2$ electrodes be maintained for NOE electrodes containing post-added $Co(OH)_2$ additives? To answer this question, we directly investigated, by means of SEM coupled with EDX, the Co distribution on fresh and partially and completely discharged Co-coated NOE electrodes (Fig. 3). For the fresh composite electrode, using EDX mapping analysis for elemental nickel, cobalt, and oxygen, we did not find, within the accuracy of the measurements, traces of cobalt or nickel oxide on the nickel foam current collector but rather found a uniform distribution of Co through the sample. In contrast, the same analysis performed on a NOE electrode discharged down to 0.2 V at a low rate (C/50) unequivocally revealed (Fig. 4) that Co is mainly concentrated on the current collector. The corresponding SEM images for the rich Co-containing sample domains near the current collector indicate the presence of large and well-shaped particles (Fig. 5) attributed to $Co(OH)_2$ that totally differ in morphology from the precursor $Co(OH)_2$ particles; these images give direct experimental proof that the cobalt compound migration to the Ni-foam current collector proceeds through a solution process.

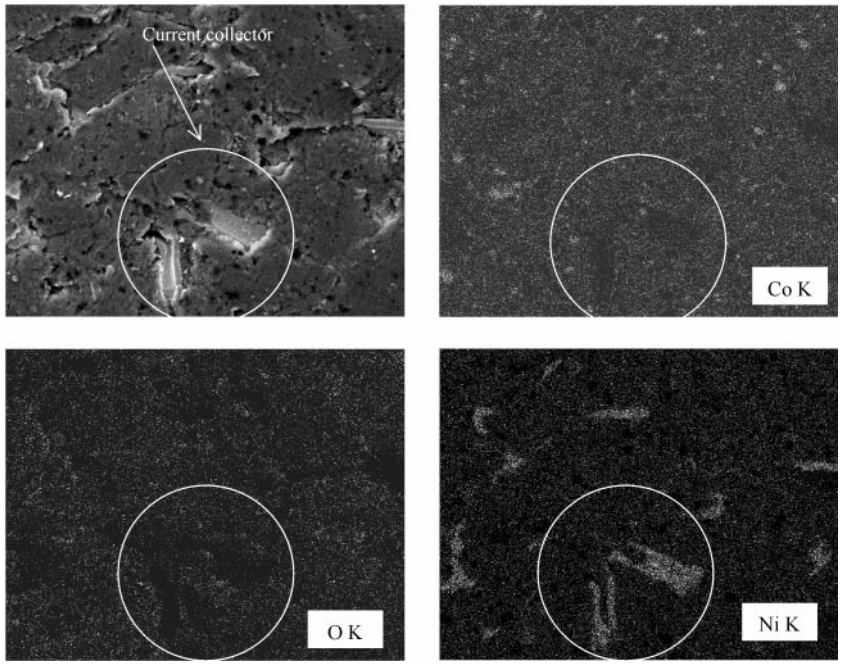

FIG. 3. Elemental X-ray analysis maps for Co, Ni, and O of the starting composite electrode containing 25 wt% of cobalt. We could observe the absence of cobalt compound over the current collector foam.

In short, the above results demonstrate that the electrochemical behavior of cobalt hydroxide when coated on a NOE electrode is similar to that of a pure $Co(OH)_2$ electrode. Thus, the previously reported schema (Fig. 6) describing the electrochemical behavior of pure $Co(OH)_2$ can directly be used to schematize the electrochemical answer of a cobalt-coated nickel hydroxide electrode during the first cycle. It should be kept in mind that a deep discharge of a Co-containing NOE electrode will seriously jeopardize its subsequent electrochemical performance.

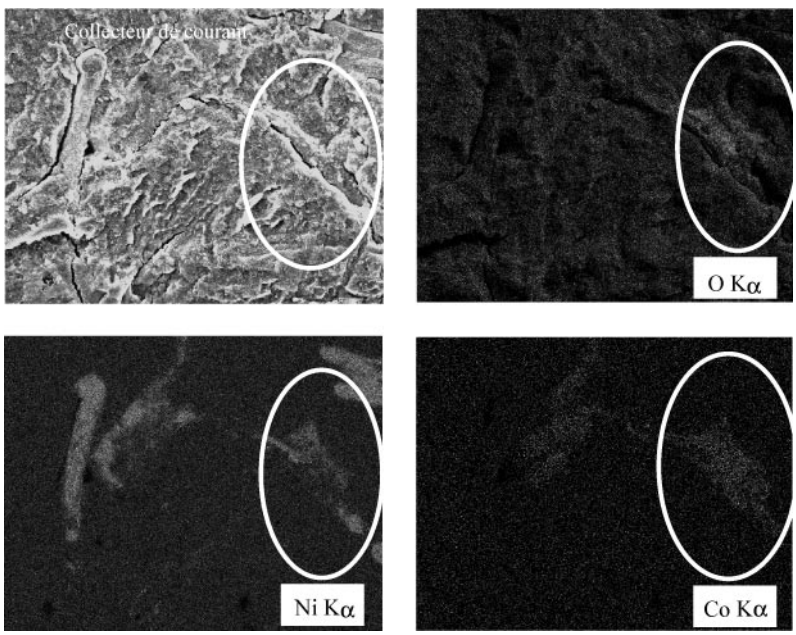

FIG. 4. Elemental X-ray analysis maps for Co, Ni, and O of a composite electrode containing 25 wt% of cobalt after a deep discharge (cutoff voltage of 0.2 V) at a rate of about C/50. We could observe the presence of cobalt compound over the current collector foam.

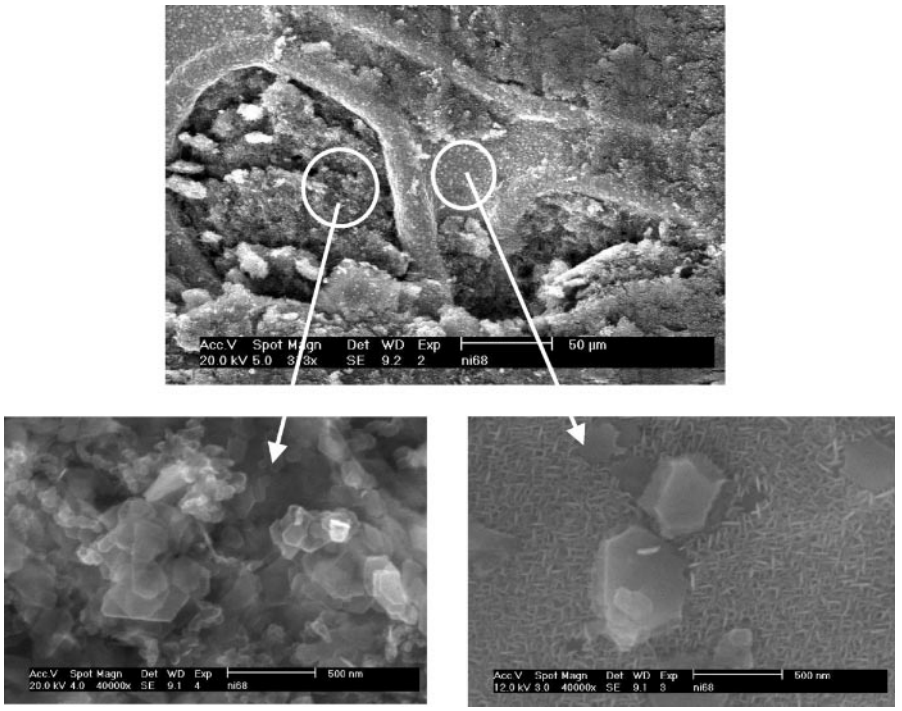

FIG. 5. Scanning electronic microscopy micrographs (FEG) of the composite electrode containing 25 wt% of cobalt compound after the deep discharge at C/50. Particles located over the nickel foam are assumed to be cobalt hydroxide pellets.

Indeed, the cobalt oxyhydroxide reduction led not only to the migration of the cobalt coating but also to the formation of a stoichiometric cobalt hydroxide, which is electrochemically inactive. It is not then purely coincidental that the majority of the commercial Ni-based batteries are potentially limited in discharge and more specifically cycled between 1 and 1.4 V for optimum efficiency. Nevertheless, postmortem microscopy analysis of NOE electrodes recovered from Ni–Cd-based cells that were cycled 1000 times within the 1–1.4 V range also revealed the growth of

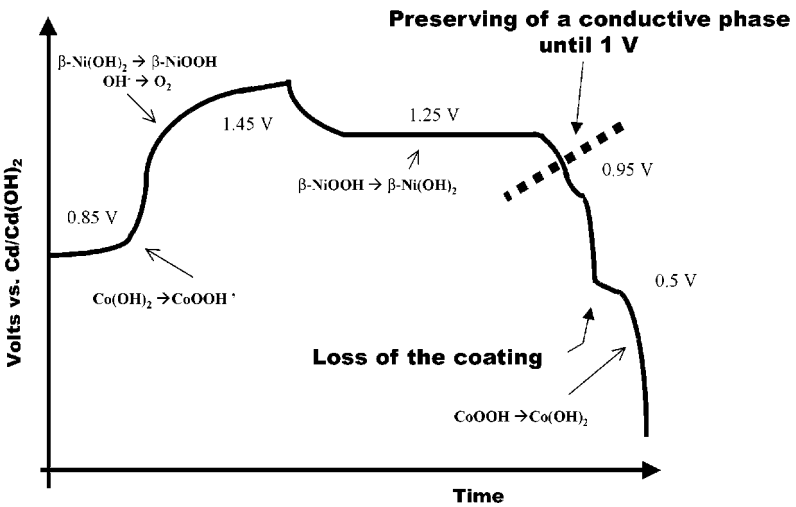

FIG. 6. Schematic representation of the first cycle for a $Ni(OH)_2$– $Co(OH)_2$ electrode.

$Co(OH)_2$ on the current collector. Thus, we decided to study Co-coated NOE electrodes evolution upon cycling within the 1.45 to 1 V range.

Effects of Heavy Cycling of a Composite Electrode

The capacity variation over 30 cycles of Co-free ($x = 0$) and Co-containing NOE electrodes ($x = 10$ and 25 wt% $Co(OH)_2$) cycled at a rate of C/5 is shown in Fig. 7. The discharges were voltage limited to 1 V while the charges were time limited (7 h 30 s being the maximum time allowed for charging). The more cobalt additive the electrode contained, the better its functioning was in terms of overall capacity and capacity retention. Interestingly, we note that the smoothness of the voltage–time discharge curve, as exemplified for the 10 wt% Co-coated NOE electrode, disappears upon cycling to the extent of a voltage-composition curve having two voltage domains separated by 50 mV (Fig. 8). The cycle-driven voltage anomaly is better highlighted by plotting the derivative curves (dx/dV vs V) that clearly reveal the appearance of a second electrochemical signature occurring at 1.20 V (Fig. 8) in addition to the normal 1.25-V peak, which corresponds to the β-NiOOH– β-$Ni(OH)_2$ redox process.

To determine the origin of the extra feature, *ex situ* X-ray diffraction measurements were performed on 10% Co-containing electrodes, in either their charged or their discharged states, after they had been cycled 5 and 50 times. By comparing the X-ray powder patterns of charged and discharged electrodes that were cycled five times we deduced, as expected, that the $\beta(II) \rightarrow \beta(III)$ was the active redox couple. In contrast, for the NOE electrode cycled 50 times we noted for the charged state (Fig. 9a) and the discharged state (Fig. 9b) the presence of the γ- and β-NiOOH phases and of the α*- and β-$Ni(OH)_2$ phases, respectively. Thus we deduced that the 1.2-V additional anomaly that developed upon cycling is the electrochemical signature of the α^*/γ phase transformation. The α^*/γ redox couple was intensely studied by Delmas *et al.* (11, 12) and Gautier (13) because of its high initial capacity (up to 350 mAh/g) that, unfortunately, could not be sustained over numerous cycles because of the progressive irreversible transformation of α-$Ni(OH)_2$ into β-$Ni(OH)_2$ upon cycling, which is the opposite of what we initially experimentally observed. These results raise several questions regarding the mechanism by which this α^*/γ phase transformation occurs and the role played by $Co(OH)_2$ in this transformation.

To test the role of Co, we first compared the incremental capacity vs potential curves after the 10th cycle for three electrodes containing 0, 10, and 25 wt% of cobalt additive (Fig. 10). On the basis of this comparison, the appearance of the 1.20-V plateau seemed to occur preferentially for NOE electrodes with high cobalt contents. To better quantify the suggested trend between the presence of the cobalt in the electrode and the appearance of the 1.20-V discharge plateau, we collected the X-ray powder patterns of the three Co-containing electrodes ($x = 0$, 10, and 25) after they had been cycled 40 times and discharged to at least 1 V (Fig. 11). It is clear that the higher the cobalt amount in the electrode, the higher the proportion of the α phase. Thus, both

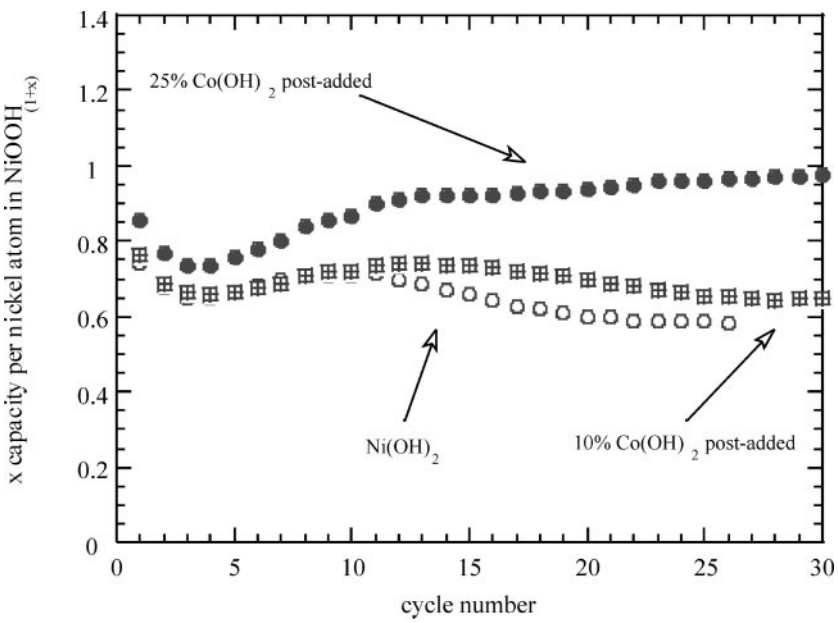

FIG. 7. Capacity versus cycle number for the NOE electrode containing various cobalt ratios (0, 10, and 25 wt%). The potential window is 1.45 to 1 V, chosen to avoid the cobalt compound migration.

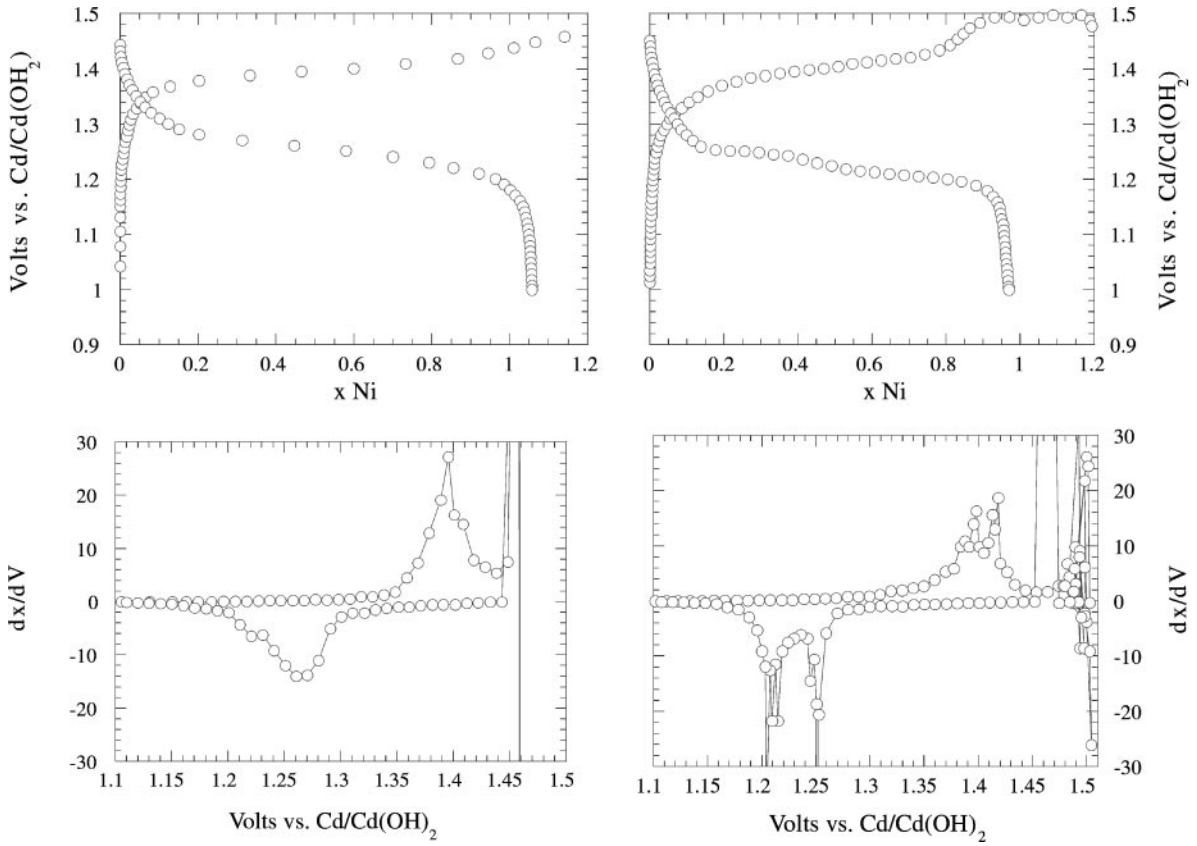

FIG. 8. Potential versus capacity curve and corresponding incremental capacity dx/dV versus potential curve of the 10th cycle for (a, b) $Ni(OH)_2$ and (c, d) $Ni(OH)_2$ with 25 wt% of $Co(OH)_2$.

electrochemical and X-ray data support that the cycle-driven growth of the α phase is directly correlated to the amount of cobalt within the NOE electrode. Knowing from the work of Delmas *et al.* (5, 11, 12) that cobalt ions are prone to stabilize the α*-$Ni_{1-x}Co_x(OH)_2$ phase, we hypothesized in the present case the growth upon cycling of a coprecipitate Ni/Co hydroxide.

To test this hypothesis we performed TEM and EDX analyses on NOE electrodes containing 25 wt% of $Co(OH)_2$, electrodes that went through 50 cycles. TEM micrographs (comparison between Figs. 12a and 12b) indicate that the particles' morphology does change during the cycling. Their edges become uneven with reduced and enlarged parts, suggesting that a part of the starting material was dissolved and precipitated back around the particle edges at various places. Furthermore, EDX measurements performed on an isolated particle indicated that it consisted of about 9 at.% Co for 91 at.% Ni "$Ni_{0.91}Co_{0.9}$" with the accuracy of the measurements being of $\pm$ 2%, while EDX analysis performed on noncycled electrodes revealed particles containing either 100 at.% of $Ni(OH)_2$ or 100% at.% of Co(CoOOH). This composition that differs from the nominal composition is further supporting evidence in favor of the growth of a Ni/Co homogenous phase. However, we are unable to determine the exact composition of this precipitate due to the fact that the core of the new "mosaic" particle (Fig. 12b) could be a partial residue of the starting $Ni(OH)_2$ particle surrounded by crystallites of the Ni/Co "coprecipitated" phase.

However, the most direct evidence for such a phase growth was obtained from potentiodynamic intermittent technique (PITT) measurements. Indeed, we demonstrated (14) that such a technique could be used as a probe to determine, depending on the potential (V_{ox}) at which the Co(II) to Co(III) oxidation occurs, whether cobalt was simply added, coated ($V_{ox} = 0.9$ V) or coprecipitated ($V_{ox} = 1.3$ V) into the nickel hydroxide matrix. We implemented this technique to determine whether Co was behaving as coprecipitated or post-added Co in a 25% Co-containing NOE electrode upon long cycling. Since the prerequisite for such a PITT test is to have Co^{2+} to start with, the cell having a 25% Co-containing electrode as the positive electrode was cycled 50 times down to a cutoff voltage of 1 V and at the end of the 50th cycle the cell

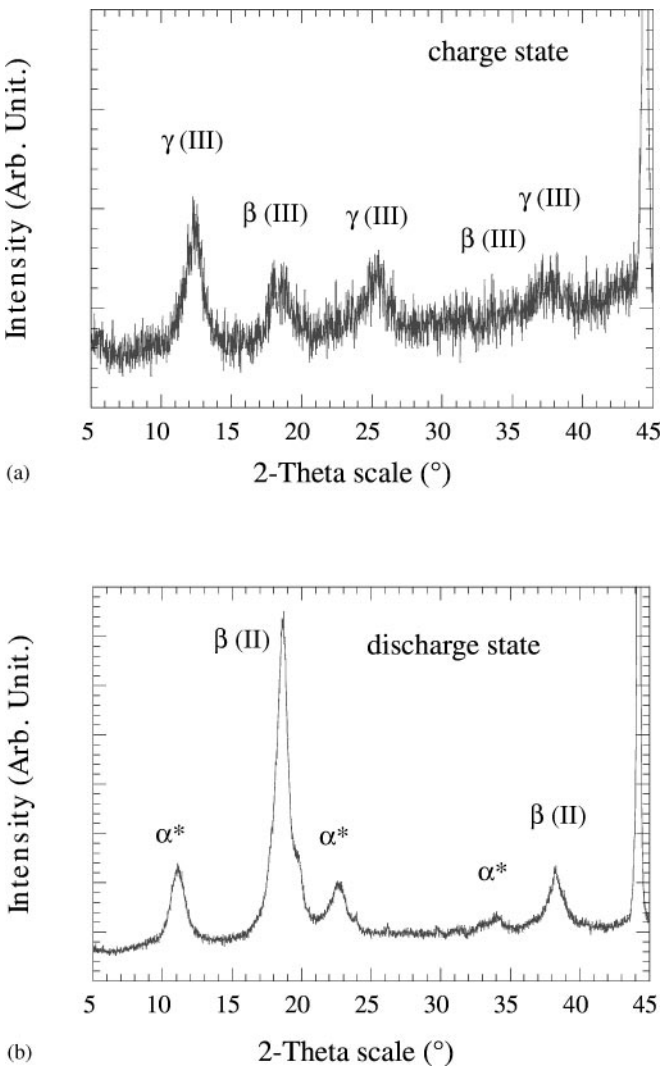

FIG. 9. X-ray diffraction patterns of the positive electrode containing 10 wt% cobalt at 1.47 V end of charge and 1 V vs $Cd/Cd(OH)_2$ after the C/5 discharge.

was fully discharged down to 0.2 V so as to reduce Co(III) onto Co(II). The chronoamperogram resulting from such a process is shown in Fig. 13. From this plot, we observed a bell-shaped current response at 1.3 V, which characterizes the biphasic oxidation detailed in our paper (14) and assigned to the presence of Co(II) intimately linked to the nickel ions in a coprecipitated Ni/Co matrix.

Thus, the results of PITT measurements and EDX analysis combined with the fact that the texture of the particle, as determined by TEM measurements, has changed supporting the conclusions that a Ni/Co coprecipitated phase has been formed and most likely through a dissolution–recrystallization process. To account for such a phase growth upon cycling, a mechanism based on the following reactions listed below that entails the formation of Co- and Ni-based complexes can be proposed.

$$Ni(OH)_2 + Co(OH)_2 \xrightarrow{1^{st}\ charge} NiOOH + CoOOH$$

$$NiOOH + CoOOH \xrightarrow[1\ V]{1^{st}\ discharge} Ni(OH)_2 + CoOOH$$

upon cycling, KOH 5N

$$Ni(OH)_2 + 6H_2O \rightarrow Ni(H_2O)_6^{2+} + 2OH^-$$

$$CoOOH + 6H_2O \rightarrow Co(H_2O)_6^{3+} + OH^- + 1/2O_2$$

Knowing that cobalt oxyhydroxide and nickel hydroxide have that same solubility in 5 N KOH (3 mg/L), one could write the overall Ni/Co coprecipitate formation as

$$(1-x)Ni^{2+}aq + 2OH^- + xCo^{3+}aq + x/n\ CO_3^{2-} + yH_2O$$

$$\rightarrow \alpha\text{-}Ni_{1-x}Co_x(OH)_2\ (CO_3^{2-})_{x/2}\ yH_2O,$$

which could simply be written as

$$Ni(OH)_2 + CoOOH \leftrightarrow Ni^{2+}\ (H_2O)_6 + Co^{3+}\ (H_2O)_6 \leftrightarrow \alpha\text{-}Ni/Co$$

reprecipitation

This mechanism is rooted in the dual dissolution of cobalt oxyhydroxide and nickel hydroxide followed by the reprecipitation of the Ni/Co phase. To ensure that the formation of a Ni/Co hydroxide complex is possible from a solution, we conducted cyclic voltammetry studies of 5 N KOH solutions containing a cobalt hydroxo complex, a nickel hydroxo complex, or both (Fig. 14). When cobalt and nickel hydroxo complexes were mixed, we observed an electrochemical signature at 1.16 V during the discharge suggesting that, while being an indirect proof, a polycomplex of nickel and cobalt and then a Ni/Co coprecipitated phase could be formed via the solution.

In the summary, we reported that when a cobalt hydroxide phase is post-added to the nickel hydroxide it transforms under standard cycling conditions into a nonstoichiometric conductive cobalt oxyhydroxide phase leading to an enhanced performance, the origin of which is nested in a better percolation path for electrons. Such an effect is at its best for commercial spherical NOE powders using a conductive cobalt oxyhydroxide coating, as long as the cycling cutoff voltage is limited to 1 V (e.g., so that CoOOH does not transform into $Co(OH)_2$. Furthermore, although the

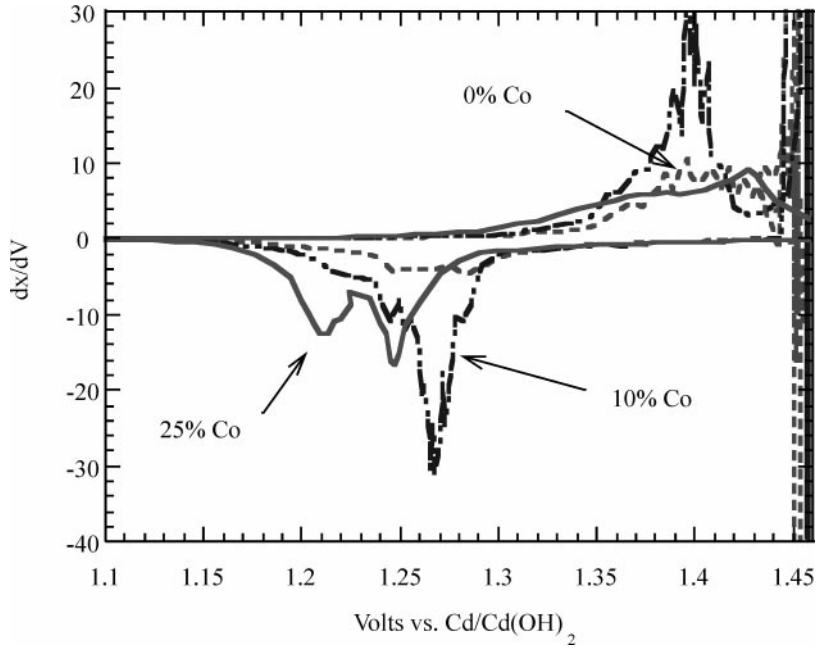

FIG. 10. Incremental capacity dx/dV versus potential curve of the 10th cycle for different cobalt content electrodes, 0, 10, and 25 wt%. We could observe the increase in the 1.20-V signature with the cobalt content.

solubility of both nickel hydroxide and cobalt oxyhydroxide in concentrated KOH electrolyte is weak ($\sim$3 mg/L) we found, to our surprise, that upon heavy cycling down to 1 V the cumulated dissolution products could lead to the formation of a Ni/Co double-lamellar hydroxide-type phase (DLH). Such a phase is electrochemically active and structurally wise similar to the α* phase. The electrochemical fingerprint of this α^*/γ redox couple is the appearance of an

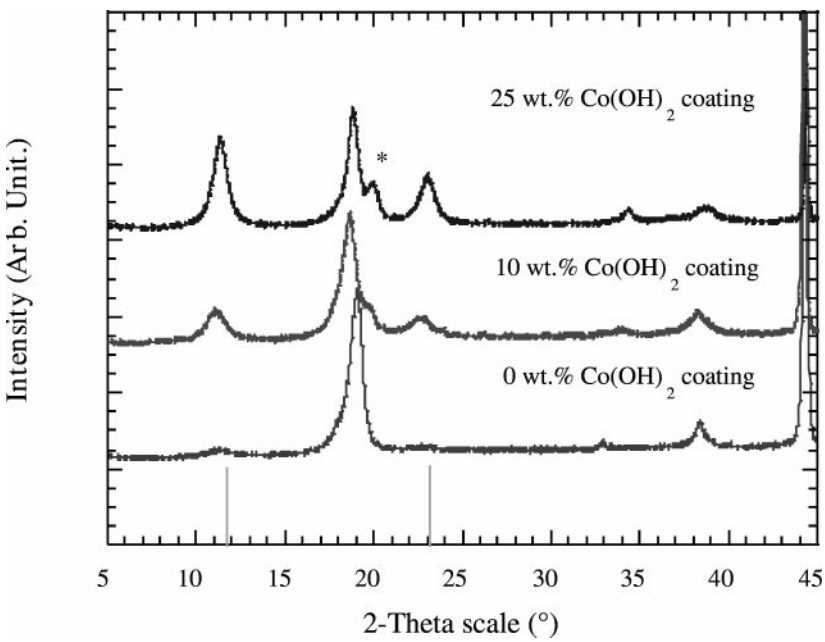

FIG. 11. X-ray diffraction patterns of discharged nickel oxyhydroxide electrodes withdraw after 50 cycles in the potential window 1.45–1 V for various cobalt-added contents: 0, 10, and 25 wt%.

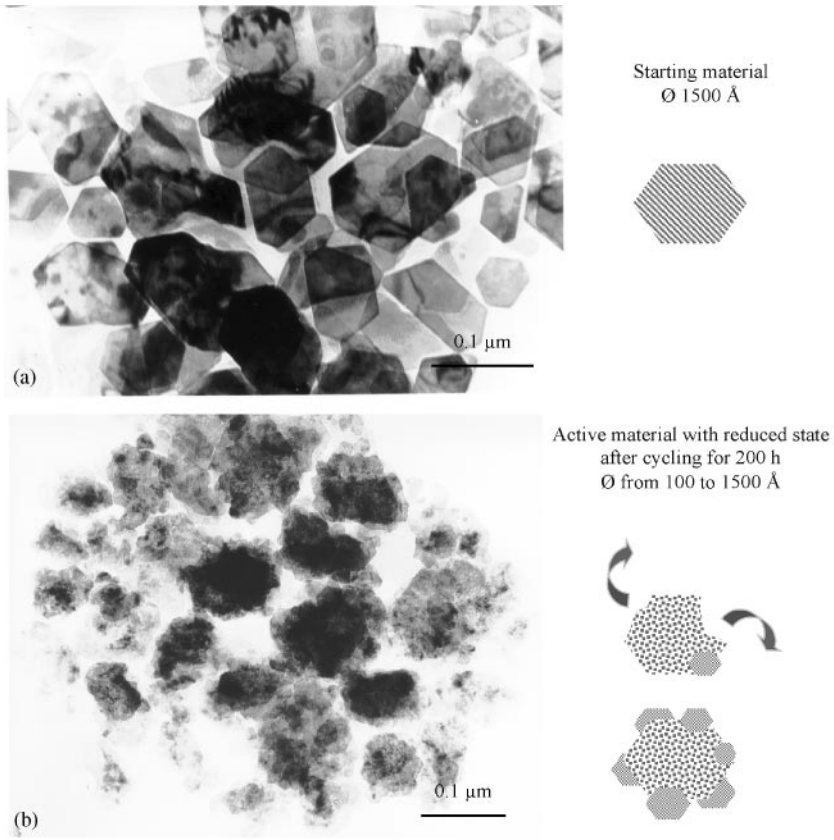

FIG. 12. TEM micrograph comparison of the starting active material $Ni(OH)_2$ + 25% $Co(OH)_2$ and the resulting active material of the same electrode after 50 cycles. A drastic dissolution process seems to have occurred.

additional 1.20-V peak on the dx/dV curve. Thus, the bending over of the capacity trace as a function of the cycle number most likely results in the sum of two opposite effects: One due to the *in situ* formation of the mixed Ni/Co γ-type phase leading to an increase in capacity and the other due to the lesser conductivity of the residual nickel hydroxide grains from the conductive cobalted phase leading to a decrease in capacity.

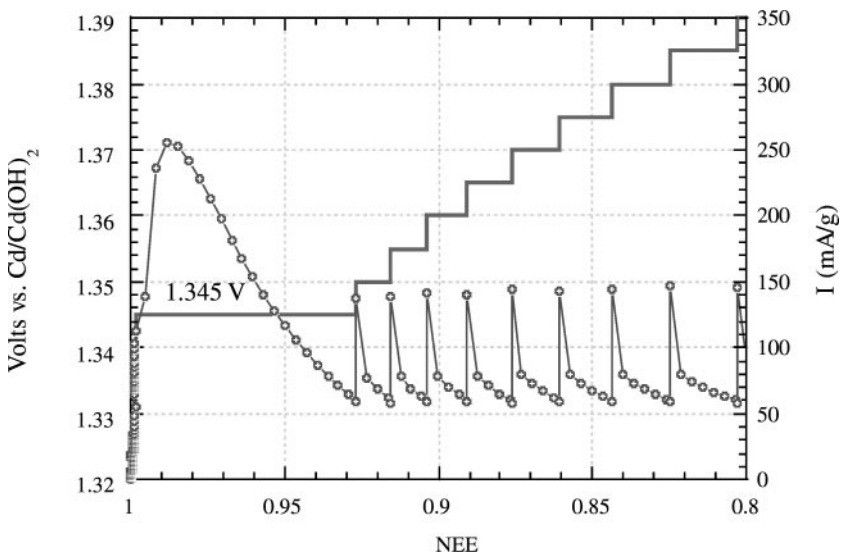

FIG. 13. Potentiodynamic first charge with galvanostatic acceleration of a cycled electrode containing 10 wt% of cobalt added after 50 cycles with a C/5 discharge, a cut-off voltage of 1 V, and a last discharge until 0.2 V.

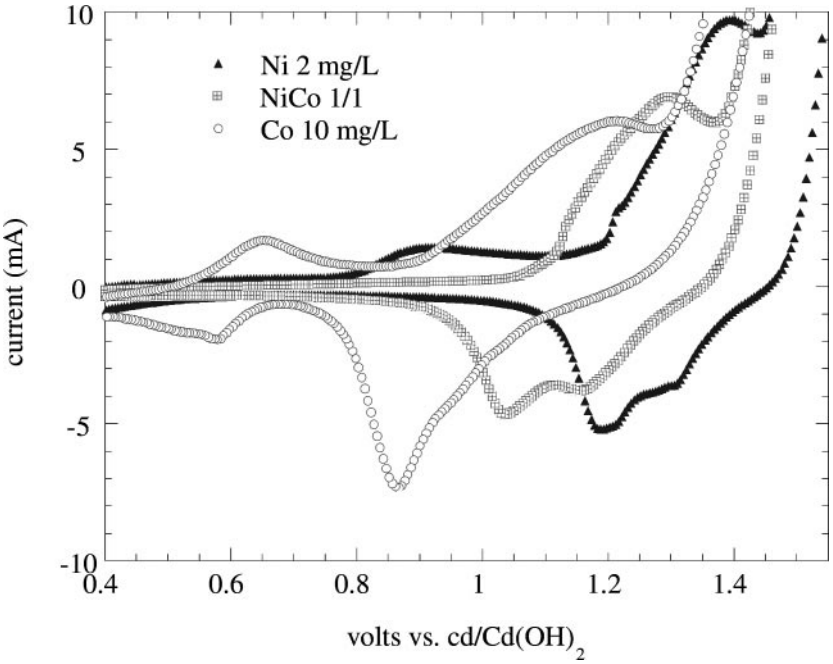

FIG. 14. Cyclic voltammetry curves for KOH solutions containing cobalt and nickel hydroxo complexes (10 mV/s, room temperature).

Let's now discuss these results in light of previous findings made by Delmas *et al.* (11, 12) and Gautier (13). Using mixed nickel/cobalt DLH-type phases as electrodes, these authors demonstrated that extended cycling (>70 cycles) down to a cutoff voltage of 1 V drives the transition from a 1.15-V peak (characterizing the α^*/γ redox potential) to a 1.28-V peak. Such a transition was shown by XRD and SEM studies to be accompanied by a cobalt demixion (e.g., the formation of CoOOH and a β-type $Ni(OH)_2$ phase from a mixed Ni/Co α^*-type phase).

Such an evolution is completely contrary to our observation using the composite electrode β-$Ni(OH)_2 + Co(OH)_2$ to start with. Indeed, the dx/dV curve reveals at the beginning of the cycling a unique peak at around 1.25 V and the gradual appearance of a second peak at 1.20 V (e.g., formation of the α^*-type phase) to the detriment of the 1.25 V peak, with these peaks still being present up to 100 cycles, the maximum we tried.

These opposite results could easily be reconciled if we bear in mind that the formation of the α^*-Ni/Co phase from the CoOOH + β-$Ni(OH)_2$ phase involves a dissolution/recrystallization process, hence the importance of solubility equilibrium in controlling the way that the reaction proceeds.

CONCLUSION

We demonstrated the positive attributes of post-added NOE electrodes when cycled down to 1 V vs $Cd/Cd(OH)_2$, but simultaneously we showed the detrimental effect of a deep discharge down to 0 V, due to the reduction of the cobalt oxyhydroxide through a solution process involving its migration to the current collector. Finally using our specified conditions, we found that upon extended cycling down to 1 V, the Co-post-added NOE composite electrode slightly evolved phase-wise with the appearance of an α^*-Ni/Co phase that formed through a solution process involving a complete reorganization of the active material. We are presently investigating to what extent such results could be extended to commercial cells that, besides their configuration, differ from the electrolyte KOH concentration.

ACKNOWLEDGMENTS

The authors thank M. Nelson for her technical help with the manuscript preparation. One of the authors (V. Pralong) is grateful to Union Minière and the Agence Nationale pour la Recherche et la Technologie (ANRT) for their financial support.

REFERENCES

1. B. E. Ezhov and O. G. Malandrin, *J. Electrochem. Soc.* **138**(4), 885 (1991).
2. M. Oshitani, T. Takayama, K. Takashima, and S. Tsuji, *J. Appl. Electrochem.* **16,** 403–412 (1986).
3. J. McBreen, W. E. O'Grady, G. Tourillon, E. Dartyge, A. Fontaine, and K. I. Pandya, *J. Phys. Chem.* **93,** 6308 (1989).
4. M. Oshitani, H. Yufu, K. Takashima, S. Tsuji, and Y. Massumaru, *J. Electrochem. Soc.* **136,** 1590 (1989).

5. M. Butel, L. Gautier, and C. Delmas, *J. Electrochem. Soc.* **122,** 271 (1999).
6. V. Pralong, A. Delahaye-Vidal, B. Beaudoin, J.-B. Leriche, and J.-M. Tarascon, *J. Electrochem. Soc.* **147**(4), 1306 (2000).
7. V. Pralong, A. Delahaye-Vidal, B. Beaudoin, B. Gérand, and J.-M. Tarascon, *J. Mater. Chem.* **9,** 955–960 (1999).
8. S. Le Bihan and M. Figlarz, *Electrochim. Acta* **18,** 123 (1973).
9. D. Guyomard and J. M. Tarascon, *J. Electrochem. Soc.* **139**(4), 937 (1992).
10. N. SacEpée, B. Beaudoin, V. Pralong, T. Jamin, J.-M. Tarascon, and A. Delahaye-Vidal, *J. Electrochem. Soc.* **146**(7), 2376 (1999).
11. C. Faure, Y. Borthomieu, C. Delmas, and M. Fourassier, *J. Power Sources* **36,** 113 (1991).
12. C. Delmas, C. Faure, and Y. Borthomieu, *Mater. Sci. Eng. B* **13,** 89 (1992).
13. L. Gautier, Thesis, University of Bordeaux I, 1995.
14. V. Pralong, Y. Chabre, A. Delahaye-Vidal, and J.-M. Tarascon, submitted for publication.